Hindawi
Geofluids
Volume 2022, Article ID 9017792, 10 pages
https://doi.org/10.1155/2022/9017792

Research Article

Numerical Study on the Relationship between the Dominant Frequency of Blasting Vibration and the Development of Plastic Zone in Cylindrical Charge

Da Liu,[1] Xiaohua Zhao,[2] Jianglin Gao,[1] Binghan Xue,[2] Xiaobin Wu,[1] Songtao Hu,[1] and Fang Chen[1]

[1]*Jiangxi Hydraulic Safety Engineering Technology Research Center, Jiangxi Academy of Water Science and Engineering, Nanchang 330029, China*
[2]*School of Water Conservancy Engineering, Zhengzhou University, Zhengzhou 450001, China*

Correspondence should be addressed to Xiaohua Zhao; zhaoxh2014@126.com

Received 23 April 2022; Accepted 25 July 2022; Published 5 August 2022

Academic Editor: Basim Abu-Jdayil

Blasting vibration is a widely studied harmful effect of rock blasting excavations. Many factors affect its dominant frequency, which makes analyzing, evaluating, and predicting it difficult. This study explored the factors influencing the dominant frequency of blasting vibrations in the case of a spherical charge. Based on symmetry, a theoretical analysis in terms of a spherical explosion source is generally sufficient to describe a cavity excited by a spherical explosion charge. The elastic cavity radius and the dominant frequency of vibration induced by the spherical blasting source are closely related. However, there is a lack of relevant research on cylindrical charges. Therefore, a calculation model for a single-hole cylindrical charge was established. There is a relationship between the corresponding dominant frequency and the range of the plastic zone. The results indicate that the dominant frequency of the blasting vibration for both cylindrical and spherical charges is closely related to the range of the plastic zone formed by the rock blasting. As the elastic cavity radius increases, both the zero-crossing and the dominant Fourier frequencies decrease, and the amplitude spectrum shifts to lower frequencies. However, increasing the cylindrical charge diameter causes more changes in the plastic zone in the direction perpendicular to the cylindrical explosive axis. Moreover, increasing the charge length causes more changes in the plastic zone along this axis. It is therefore difficult to identify a unique dimensional parameter that characterizes the range of the plastic zone formed by the blasting. Because the plastic zone around a cylindrical charge is less regular than around a spherical charge, the charge weight Q is a more favorable parameter than the elastic cavity radius a when used as the main influencing factor and in an attenuation analysis for the dominant frequency of cylindrical charge blasting.

1. Introduction

As an efficient excavation method, borehole blasting is easy to induce harmful vibration effects, which has always been the focus of attention [1–3]. The dominant frequency induced by cylindrical charge is an important index to characterize blasting vibration [4, 5], but the theoretical research is not sufficient compared with spherical charge. Therefore, to fully understand the vibration characteristics of cylindrical charge qualitatively and quantitatively, it is often necessary to learn from the relevant spherical charge theory [6]. Previous studies have demonstrated that there are two stages of blasting vibration effect induced by spherical charge. The first stage is the initial state of explosive expansion, where the energy released by the explosive expands symmetrically in all directions, and P wave is generated, causing compression deformation in the surrounding rock mass. The second stage is the roof-like uplift caused by the expansion of soil within a certain epicenter distance due to the residual pressure of explosive gas in the spherical cavity, which is considered as the elastic vibration in the near region. For the spherical explosion source, due to the spherical symmetry of the explosion load, the problem can

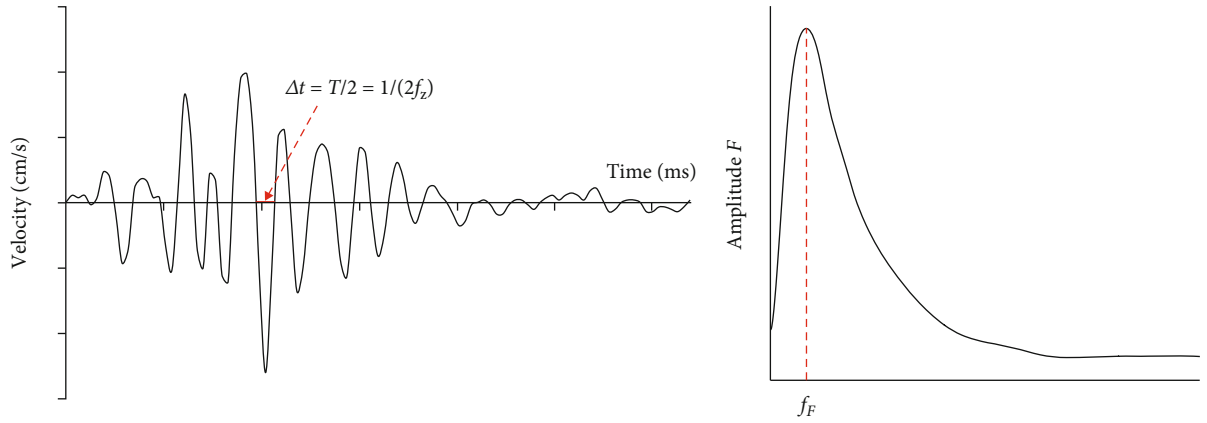

(a) Velocity–time histories of blasting

(b) Amplitude spectrum

Figure 1: Typical waveform and spectrum of blasting vibration.

be simplified to a one-dimensional problem, and the solution of the problem can be obtained through analytical calculation [7] so that the relationship between the vibration spectrum and the radius of the plastic zone can be analyzed and obtained. However, for cylindrical charge, the analytical solution of its dominant frequency is difficult to obtain due to the influence of many factors such as charge structure, explosion energy release form, and free surface [8, 9].

According to the degree of damage to the rock mass around the borehole blasting, it can be simply divided into crushed zone, cracked zone, and elastic formation zone [10]. In fact, the blasting damage of rock mass is a complex dynamic accumulation process. When discriminating the range of rock damage, most of the current methods to evaluate rock blasting damage are based on numerical modeling [11]. Grady [12] proposed an isotropic damage model for rock blasting, which uses a scalar to describe the deterioration of rock stiffness and assumes that the number of cracks obeys the two parameter Weibull distribution. Yang et al. [13] believe that the crack can propagate only when the bulk strain is greater than a certain value and proposed the concept of fracture probability, which is introduced in the definition of damage variable. Ma [14] introduced the Johnson-Holmquist (J-h) material model into LS-DYNA to simulate the rock fracture damage process caused by blasting.

To obtain the range of rock blasting damage area, most methods are trying to calculate the peak particle velocity (PPV) produced by the detonating charge compared against a PPV that is known or adopted (most of the time based on site-specific field tests) that will produce some damage in the rock or rock mass [15]. Holmberg-Perssion [16] assumes that the cylindrical charge is regarded as a small section connected in series, and the PPV distribution in the rock mass can be obtained by combining each small section of charge. Based on the cylindrical wave theory and the wavelet theory of spherical wave and long cylindrical charge, Hustrulid and Lu [17] deduced the theoretical formula for the attenuation of peak vibration velocity of blasting vibration particles by considering the detonation velocity of explosives from the viewpoint proposed by Starfield [18]. Most of the studies combine the damage range of rock with PPV, and generally, the larger the PPV induced by rock blasting, the larger the range of cracked zone caused by blasting. In fact, similar to PPV, the dominant frequency of blasting vibration is also an important parameter to characterize blasting vibration [19], which has two most commonly used definitions, including zero-crossing frequency f_z (the frequency corresponding to the peak vibration period) and Fourier frequency f_F (the frequency corresponding to the maximum amplitude in the spectrum), shown in Figure 1. And the dominant frequency is also closely related to the damage range formed by rock blasting [20]. However, there is much less research on the relationship between the dominant frequency of blasting vibration and the range of cracked zones caused by blasting. Therefore, through the research, it can provide some meaningful perspectives for exploring the propagation characteristics and attenuation characteristics of the dominant frequency of blasting vibration.

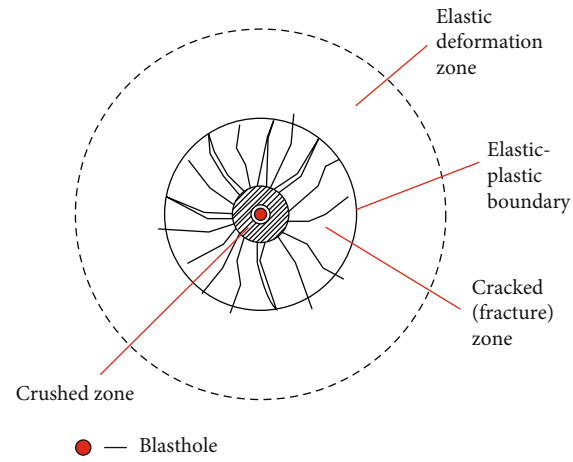

Figure 2: Damage zones surrounding a spherical detonation.

On the basis of the stress wave excited by spherical cavity explosion in an elastic rock mass, the theoretical solution of spherical wave propagation and the velocity spectrum are analyzed. By establishing the dynamic finite element model of

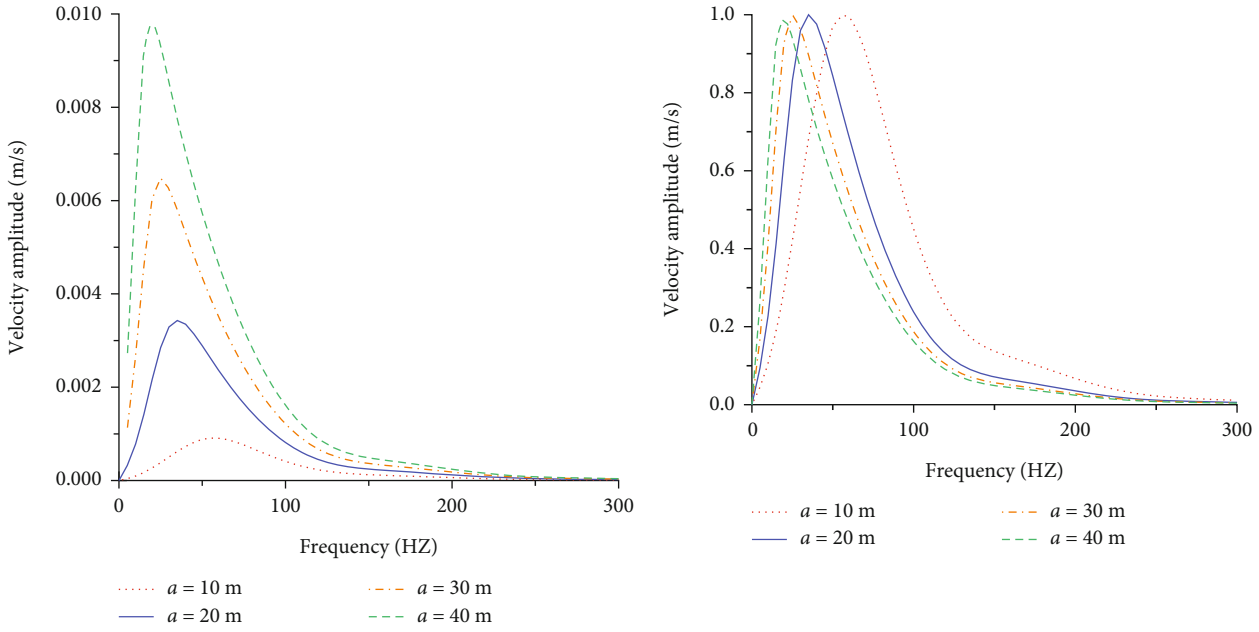

(a) Velocity amplitude spectrum

(b) Normalized to the peak value of the spectrum

Figure 3: Amplitude spectrum variation law of different elastic cavity radius.

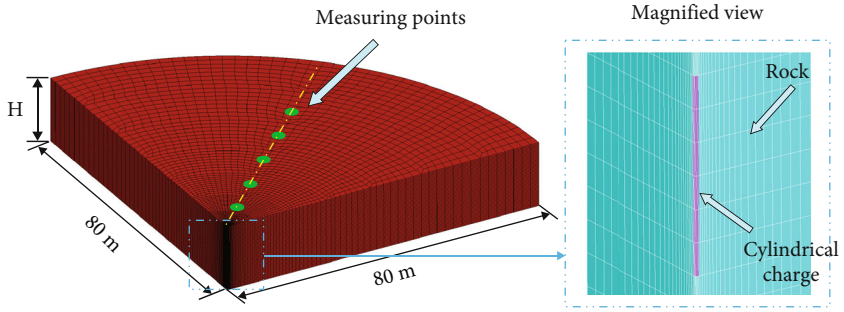

Figure 4: Quarter cylinder finite-element model.

single borehole cylindrical charge, the distribution characteristics of rock blasting cracked zone are analyzed, and the numerical relationship between the cracked zone of blasting and the dominant frequency is explored, which is helpful to understand the factors affecting the dominant frequency of blasting vibration by cylindrical charge.

2. Relationship between the Cracked Zone and the Dominant Frequency

The explosive blasting causes a large transient impact load acting on the rock, and the energy released by the explosive propagates outward in the form of stress wave. The regions encountered by a blasting stress wave propagating away from the blasting center can be approximately classified as the crushed, cracked, and elastic areas, according to the degrees of damage in the rock, and the propagation properties of shock, stress, and seismic waves vary accordingly. In the crushed zone, the rock is crushed because the pressure caused by the blasting load greatly exceeds its compressive strength. In the cracked (fracture) zone, the circumferential tensile stress of the rock mass often exceeds its tensile strength; the rock mass also undergoes an irreversible tensile deformation. In the elastic deformation zone, the load on the rock mass is only sufficient to cause elastic vibration and not plastic deformation. The blasting damage zone of the rock mass is illustrated in Figure 2.

To facilitate the analysis, the nonelastic zones (crushed zone and cracked (fracture) zone) near the blasthole are generally regarded as the equivalent blasting source, in which the elastic-plastic boundaries are applied on the blasting load [21–23]. Therefore, the theoretical solution of an elastic wave excited by a spherical cavity in an elastic medium can be adopted [7].

Introducing a potential function φ to represent the radial displacement

$$u = \frac{\partial \varphi(r,t)}{\partial r}. \tag{1}$$

Assuming the load function acting on the inner wall of the spherical cavity is $p(t)$,

Table 1: Calculation parameters of JWL equation of state for explosives.

Material	Density (g/m^3)	V (m/s)	CJ pressure (Pa)	A (GPa)	B (GPa)	R_1	R_2	ω
Explosion	1×10^3	3600	3.24×10^9	214	0.18	4.2	0.9	0.15

Table 2: Calculation parameters of rock materials.

Material	Elastic modulus (GPa)	Density (g/m^3)	Poisson's ratio	Shear modulus (GPa)	Bulk modulus (GPa)	Yield stress (MPa)
Rock	20	2400	0.24	8.06	12.8	40

Table 3: The radius of the middle section under different charge diameters.

Charge diameter d (mm)	Charge length l (m)	Charge weight Q (kg)	The radius of the middle section (m)
90	8	50.89	1.96
110	8	76.03	2.59
130	8	106.19	3.19

Table 4: Radius of plastic zone under different charge diameters.

Charge diameter d (mm)	Charge length l (m)	Charge weight Q (kg)	The radius of the middle section (m)
110	6	57.02	2.59
110	8	76.03	2.59
110	10	95.03	2.59

$$\varphi(r,t) = -\frac{a}{\rho\omega r}\int_0^s p(s-t)e^{-\eta\tau}\sin(\omega\tau)d\tau, \tag{2}$$

$$s = t - \frac{r-a}{C_P}, \tag{3}$$

$$\eta = \frac{1-2\nu}{1-\nu}\frac{C_P}{a}, \tag{4}$$

$$\omega = \frac{\sqrt{1-2\nu}}{1-\nu}\frac{C_P}{a}, \tag{5}$$

where $p(t)$ is the blasting load acting on the elastic cavity, λ and μ are the constants of lame, ν is Poisson's ratio, ρ is the density, and C_p is the longitudinal wave velocity. a is the radius of the elastic cavity (cracked zone). ω is the phase of the function φ, which is also the natural frequency of the equivalent system.

When the dynamic load of stress waves over time is adopted in the form

$$p(t) = \begin{cases} 0 & t<-\tau_1, \\ \sigma_{\max}(1+t/\tau_1) & -\tau_1 \le t \le 0, \\ \sigma_{\max}(1-t/\tau_2) & 0 \le t \le \tau_2, \\ 0 & t > \tau_2, \end{cases} \tag{6}$$

where $\sigma_{\max}$ is the peak value of blasting load, τ_1 is the rising time of blasting load, and τ_2 is the time of blasting load reduction from peak to zero.

By means of Fourier transform, the velocity spectrum of blasting vibration in elastic rock mass due to the action of $p(t)$ on the elastic boundary can be obtained as follows:

$$F(\omega) = \frac{|S_\sigma(j\omega)|a\omega C_p\sqrt{C_p^2 + r^2\omega^2}}{4\mu r^2\sqrt{(C_p/a)^4 + [1-(\lambda+2\mu)/2\mu]\omega^2(C_p/a)^2 + [(\lambda+2\mu)/4\mu]^2\omega^4}},$$
$$|S_\sigma(j\omega)| = \frac{\sigma_{\max}}{a_e b_e \tau\omega^2}\left[1 + a_e^2 + b_e^2 + 2a_e b_e\cos\omega\tau - 2(a_e\cos b_e\omega\tau + b_e\cos a_e\omega\tau)\right]^{1/2}, \tag{7}$$

where $\tau = \tau_1 + \tau_2$, $a_e = \tau_1/\tau$, and $b_e = \tau_2/\tau$.

The same rock mass parameters are selected: density $\rho = 2700\,\text{kg/m}^3$, Poisson's ratio = 0.22, peak value of blasting load $\sigma = 50\,\text{MPa}$, duration of blasting load $\tau = 10\,\text{ms}$, and rising time of blasting load $\tau_1 = 2\,\text{ms}$. The influence of elastic cavity radius on the blasting vibration spectrum is analyzed

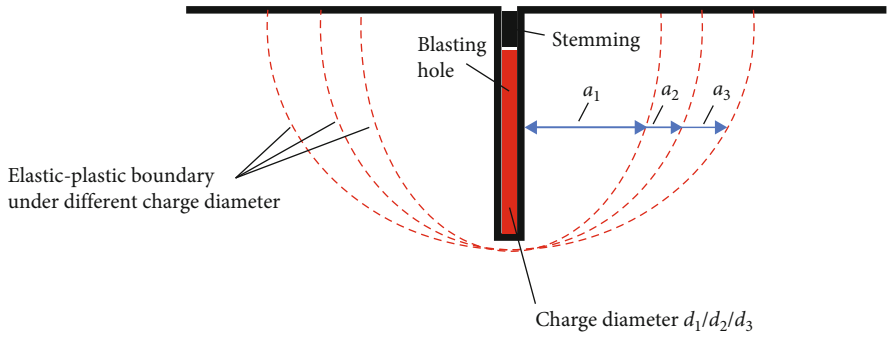

Figure 5: Elastic-plastic boundary under different charge diameter.

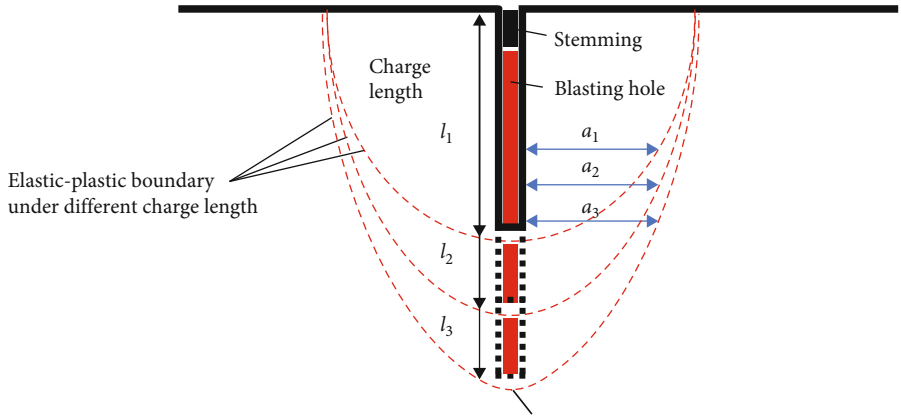

Figure 6: Elastic-plastic boundary under different charge lengths.

by substituting the rock parameters into the formula. The velocity amplitude spectra corresponding to different elastic cavity radius (elastic cavity radius $a = 10$ m, 20 m, 30 m, 40 m, 50 m) are plotted in Figure 3(a), and the normalized velocity amplitude spectra are plotted in Figure 3(b).

As shown in Figure 3, increasing the radius of the elastic cavity increases the amplitude of the vibration velocity spectrum and shifts the peak toward lower frequencies. The dominant Fourier frequency decreases with increasing radius of the elastic cavity.

3. Relationship between the Plastic Zone and the Dominant Frequency in Cylindrical Charge

3.1. Range of Plastic Zone. Under the condition of cylindrical charge, when the external load of the rock around the explosive reaches a certain value, the stress exceeds the yield strength of the rock, which brings irreversible plastic deformation. Cylindrical charge is different from the spherical charge that the plastic zone is not an approximate spherical zone, and the evolution radius of the plastic zone is not easy to define. In this study, the plastic deformation range of rock around the borehole is compared under different working conditions, and the plastic radius of the middle section of charge length with the bottom initiating cylindrical charge (hereinafter referred to as "the radius of the middle section") is taken for comparison under all different working conditions. In LS-DYNA program, when the equivalent stress is equal to the yield stress of the material, it is also used as the judgment standard for the material to enter plastic deformation. The yield criterion at coordinates i, j is as follows:

$$\frac{1}{2}s_{ij}s_{ij} - \frac{1}{3}\sigma_s^2 = 0, \tag{8}$$

where $s_{ij} = \sigma_{ij} - \sigma_m\delta_{ij}$ is the deviatoric stress tensor, $\sigma_{m=}1/3_{(\sigma_{11+}\sigma_{23+}\sigma_{33})}$ is the average stress, σ_s is the yield stress of rock, when the plastic deformation of rock occurs, and $\sigma_{11}, \sigma_{22}, \sigma_{33}$ is the first, second, and third principal stresses, respectively.

$$\bar{\sigma} = \frac{1}{\sqrt{2}}\sqrt{(\sigma_1 - \sigma_2)^2 + (\sigma_2 - \sigma_3)^2 + (\sigma_3 - \sigma_1)^2}. \tag{9}$$

Under the action of explosion load, the equivalent stress of rock $\bar{\sigma}$ is greater than the yield stress of rock σ_s.

3.2. Numerical Model and Calculation Conditions. The blasting process of a cylindrical charge in an infinite rock mass was simulated numerically using a finite-element model and numerically analyzed using the LS-DYNA software. The model represents a quarter cylinder of radius 80 m, as shown in Figure 4.

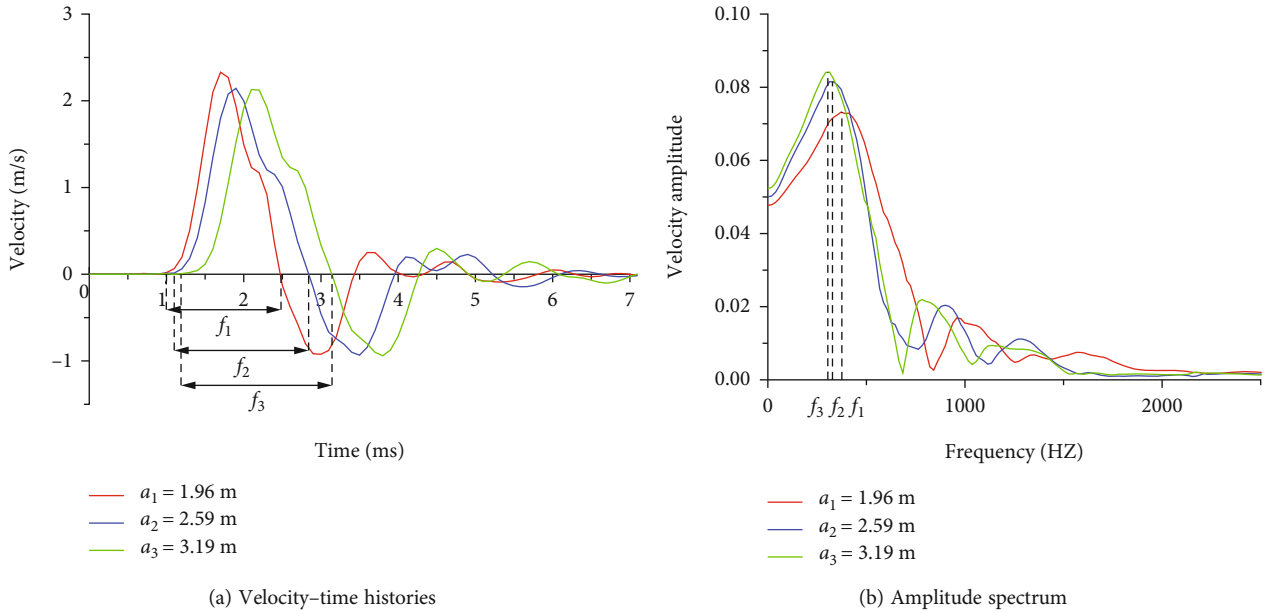

(a) Velocity–time histories

(b) Amplitude spectrum

Figure 7: Waveforms and spectra of the elastic-plastic boundary under different charge diameters.

Table 5: Radius of plastic zone under different charge diameters.

Charge diameter d (mm)	Charge weight Q (kg)	The plastic range radius of the middle section a (m)	Zero-crossing dominant frequency (Hz)	Fourier dominant frequency (Hz)
90	50.89	1.96	322.6	371.8
110	76.03	2.59	270.3	332.7
130	106.19	3.19	263.2	313.1

The dynamic impact of explosives is simulated by using the fluid-solid coupling algorithm, and the relationship between pressure and volume during the explosion is calculated by combining with JWL equation of state, in which the calculation parameters of the emulsion explosives used are shown in Table 1.

V is the velocity of detonation, A and B are the product JWL coefficient, R_1 and R_2 are the unreacted JWL coefficient, and CJ pressure is the initial pressure.

The rock mass is simplified as an isotropic ideal elastic-plastic material simulated by the bilinear elastic-plastic model in Table 2.

The development of the elastic cavity radius was analyzed by changing the radius and length of the charge, which are the dimensions commonly used in the context of foundation excavation in hydraulic engineering. The variations of the elastic cavity radius for different charge parameters are listed in Tables 3 and 4.

Under the condition of a constant charge length, we calculated the radii of the middle section formed by blasting, for charge diameters $d = 90$, 110, and 130 mm.

Under the condition of a constant charge diameter, we calculated the radii of the middle section formed by blasting, for charge length $l = 6$ m, 8 m, and 10 m.

As shown in Table 3, the plastic radius of the middle section of the charge length increases with the charge diameter between 90 and 130 mm. According to Table 4, the range of the plastic zone increases when the charge diameter remains constant at 110 mm while the charge length increases from 6 to 10 m. However, its size increases mainly along the axial direction of the cylindrical charge, and the plastic radius of the middle section for charge lengths a_1, a_2, a_3 shows no significant change.

Figures 5 and 6 suggest that an increase in the charge diameter and the charge length increases the range of the plastic zone. An increase in the charge diameter tends to increase the range of the plastic zone in the direction perpendicular to the explosive axis, and an increase in the charge length tends to increase the range of the plastic zone along the explosive axis direction. Therefore, the diameter of the plastic range of the cylindrical charge is more difficult to define owing to the shape of the charge in contrast to a spherical charge.

3.3. Analysis Results under Different Charge Diameters. Measuring points at the elastic-plastic boundary in the middle section were selected for analysis, in the case of different charge diameters $d = 90$, 110, and 130 mm. The waveform and frequency spectrum at these measuring points are compared and analyzed in Figure 7 and Table 5.

The plastic radius of the middle section shows little change for charge lengths $l = 6$, 8, and 10 m. Measuring points on the elastic-plastic boundary of the middle section

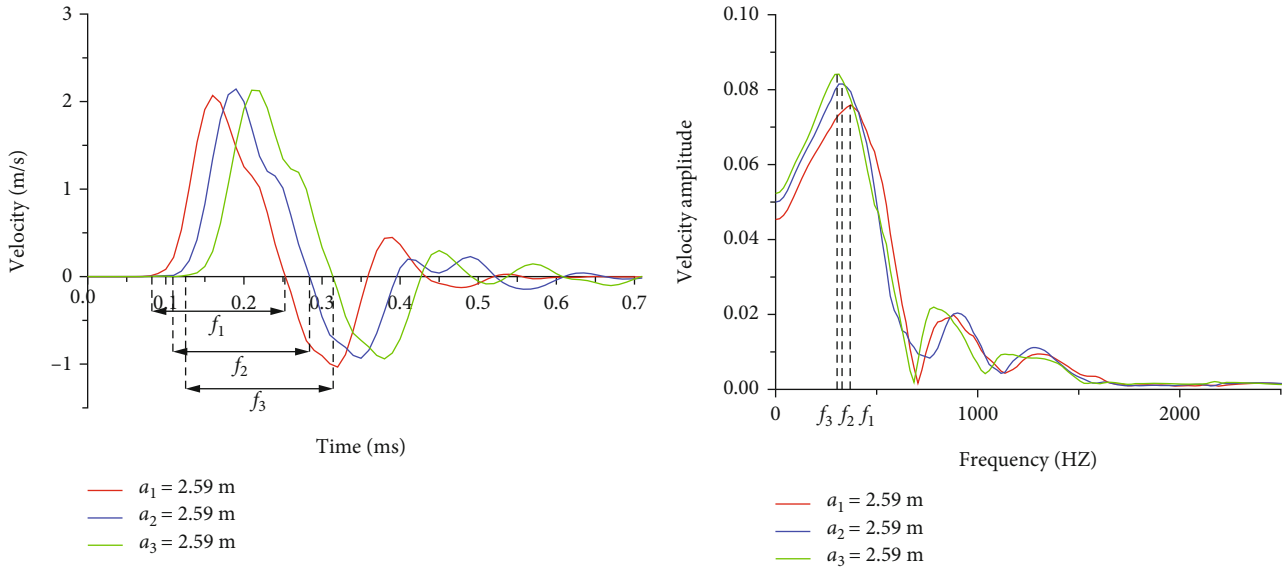

(a) Velocity–time histories

(b) Amplitude spectrum

Figure 8: Waveforms and spectra of the elastic-plastic boundary under different charge diameters.

Table 6: Radius of plastic zone under different charge length.

Charge length l (m)	Charge weight Q (kg)	The plastic range radius of the middle section a (m)	Zero-crossing dominant frequency (Hz)	Fourier dominant frequency (Hz)
6	57.02	2.59	294.1	371.8
8	76.03	2.59	270.3	332.7
10	95.03	2.59	263.2	313.1

were selected for analysis, and the corresponding waveforms and spectra are compared and analyzed in Figure 8 and Table 6 for various working conditions.

When increasing either the charge diameter or length, the plastic zone range also increases. However, changing the charge diameter and length causes the plastic zone to change in two different directions relative to the explosive geometry. This is a consequence of the more complex charge structure and load energy-release mechanism pertaining to a cylindrical charge, compared to a spherical charge. Therefore, the diameter of the plastic zone induced by the cylindrical charge is more difficult to define than in the case of a spherical charge.

Figures 7 and 8 suggest that increasing the charge diameter and length causes an increase in the range of the plastic zone and a decrease in the zero-crossing dominant frequency and in the dominant Fourier frequency. This is generally consistent with the results obtained for a spherical charge. However, the charge diameter and the charge length cause the plastic zone to change in two different directions relative to the explosive geometry. Specifically, an increase in the charge diameter causes an increase in the plastic range in the direction perpendicular to the explosive axis, and an increase in the charge length causes an increase in the plastic range along the explosive axis.

According to Equation (5), the dominant frequency of a blasting vibration often has a proportional relationship with C_p/a or C_p/Q. Most existing formulas for this frequency show C_p/a or C_p/Q as the proportionality factor [19, 24, 25]. Under the condition of spherical charge, the charge weight Q and the radius of elastic cavity a are interchangeable according to the relationship expressed as follows:

$$Q = \frac{4}{3}\pi a^3 q, \tag{10}$$

where q is the unit explosive consumption of rock.

The plastic zone radius a of a cylindrical charge is challenging to determine in an actual blasting process. (For example, as shown in Table 6, for a constant charge diameter and a charge length varying from 6 to 10 m, the plastic radius of the middle section does not change significantly.) It is therefore often replaced by the charge weight Q. A reasonable correlation is observed between the radius of the plastic zone and the dominant frequency of the cylindrical charge in Figures 9 and 10. However, owing to the complexity of the definition of plastic zone, the charge weight Q is a more favorable parameter than the elastic cavity radius a when used as the main influencing

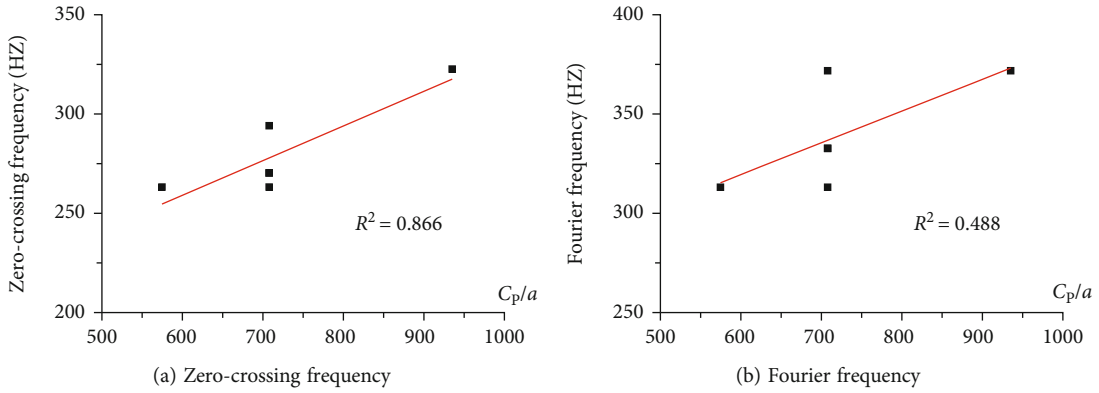

(a) Zero-crossing frequency (b) Fourier frequency

Figure 9: Linear fitting relationship between the dominant frequency and C_p/a.

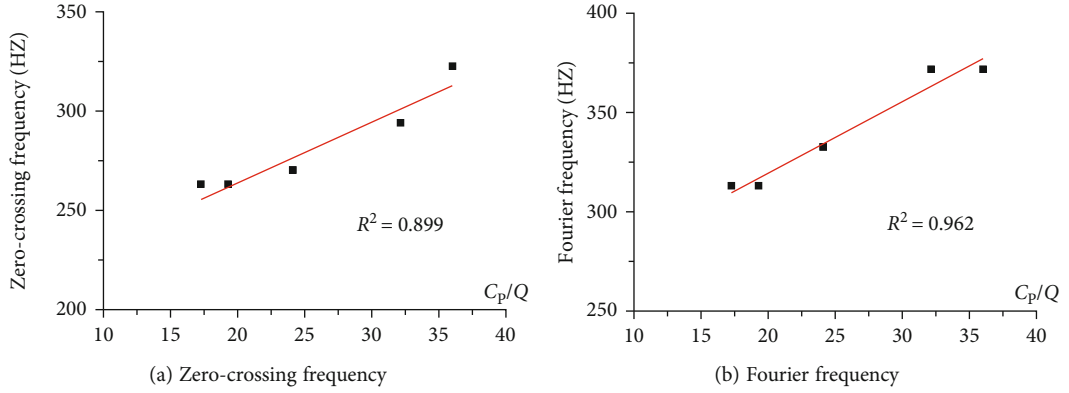

(a) Zero-crossing frequency (b) Fourier frequency

Figure 10: Linear fitting relationship between the dominant frequency and C_p/Q.

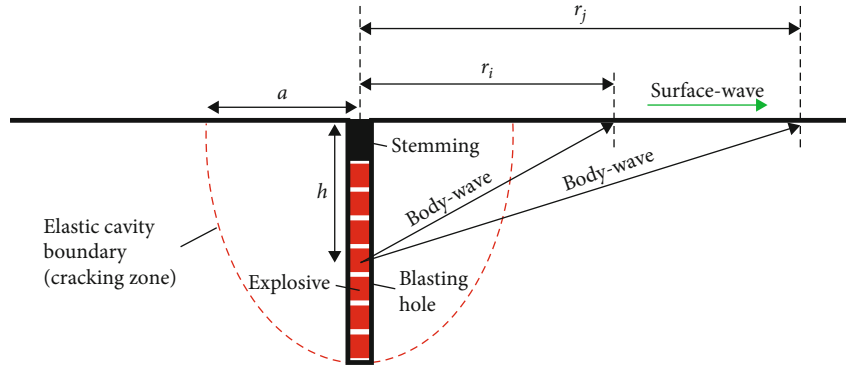

Figure 11: Schematic diagram of single-hole blasting.

factor and in the attenuation analysis of the dominant frequency of cylindrical charge blasting.

4. Discussion

Explosive blasting in rock forms a rock damage area. For cylindrical charge, there have been many studies on the definition and range of rock damage, which are different according to the rock damage criteria. For instance, Xayyraed [26] shows that when blasting a single hole in a semi-infinite rock medium with a known blasting load, the crushed zone radius r_1 and fractured (cracked) zone radius r_2 take the form

$$r_1 = \left(\frac{\rho_r C_P^2}{5\sigma_c}\right)^{1/2} \left(\frac{P}{\sigma}\right)^{1/4} a, \tag{11}$$

$$r_2 = \left[\frac{\mu P}{(1-\mu)\sigma_t}\right]^{1/\beta} a, \tag{12}$$

where μ is the Poisson ratio, C_p is the P wave velocity of the rock mass, σ_c and σ_t are the unconfined compressive strength

and tensile strength of the rock, σ is the compressive strength of the rock under multiaxial stress, P is the radial blasting load, and β is the attenuation exponent of the stress wave.

In Equations (10) and (12), the range of rock blasting damage area is comprehensively affected by rock mechanical parameters, blasting load, and charge weight (diameter). It can be seen that the range of rock plastic area is a more comprehensive index for the influencing factors of blasting vibration dominant frequency, compared with charge weight. However, it is not easy to characterize the range of rock damage zone for cylindrical charge.

In the process of excitation and propagation of blasting seismic waves, affected by the form of explosion source, the types and dominant components of blasting-induced seismic waves will be different. Different types of seismic waves will inevitably lead to the differences of blasting vibration spectrum and dominant frequency due to their differences in propagation speed and attenuation characteristics. According to the different propagation paths of the wave, it can be divided into body wave and surface wave. The propagation of body wave in rock mass can be divided into compressive wave (P wave) and shear wave (S wave), as shown in Figure 11. In terms of the existence of the surface free surface, the surface wave (S wave) will also appear on the free surface of the semi-infinite space, which further increases the complexity of analyzing the dominant frequency of cylindrical charge blasting.

5. Conclusion

In this study, the numerical relationship between the elastic cavity radius and the dominant frequency induced by cylindrical charge has been explored. It has been found that

(1) with the increase of the elastic cavity radius, the zero-crossing and the Fourier dominant frequency decreases, and the amplitude spectrum shifts to the low frequency part, which is similar to the regulation of spherical charge obtained by theoretical analysis

(2) both the increase of charge diameter and charge length will increase the plastic zone induced by cylindrical charge, but as a result of the more complex charge structure and load energy release mechanism of cylindrical charge compared with spherical charge, the charge diameter and charge length will cause the plastic zone to change in the different directions of the explosive

(3) the range of plastic zone of cylindrical charge also has an approximate logarithmic relationship with the dominant frequency. However, since the plastic zone of cylindrical charge is less regular than that of spherical charge, the charge weight Q is a more favorable parameter compared with the elastic cavity radius a when used as the main influencing factor and attenuation analysis on the dominant frequency of cylindrical charge blasting

Data Availability

The data that support the findings of this study are available from the corresponding author upon reasonable request.

Conflicts of Interest

The authors declare that they have no conflicts of interest.

Acknowledgments

This work is supported by the Natural Science Foundation of Jiangxi Province (20212BAB214044 and 20204BCJ23002), supported by the National Natural Science Foundation of China (51779190, 51779193, and 52009126), and supported by the Jiangxi Provincial Department of Water Resources Foundation (202224ZDKT08). The authors wish to express their thanks to all supporters.

References

[1] J. Henrych, *The Dynamics of Explosion and Its Use*, Elsevier Scientific Publishing Company, New York, 1979.

[2] C. H. Dowding, *Construction Vibrations*, Prentice-Hall, Upper Saddle River, NJ, 1966.

[3] P. K. Singh and M. P. Roy, "Damage to surface structures due to blast vibration," *International Journal of Rock Mechanics and Mining Sciences*, vol. 47, no. 6, pp. 946–961, 2010.

[4] J. H. Yang, W. B. Lu, Q. H. Jiang, C. Yao, S. Jiang, and L. Tian, "A study on the vibration frequency of blasting excavation in highly stressed rock masses," *Rock Mechanics and Rock Engineering*, vol. 49, no. 7, pp. 2825–2843, 2016.

[5] J. R. Zhou, W. B. Lu, P. Yan, M. Chen, and G. H. Wang, "Frequency-dependent attenuation of blasting vibration waves," *Rock Mechanics and Rock Engineering*, vol. 49, no. 10, pp. 4061–4072, 2016.

[6] C. Knock and N. Davies, "Blast waves from cylindrical charges," *Shock Waves*, vol. 23, no. 4, pp. 337–343, 2013.

[7] R. F. Favreau, "Generation of strain waves in rock by an explosion in a spherical cavity," *Journal of Geophysical Research*, vol. 74, no. 17, pp. 4267–4280, 1969.

[8] X. Jiang, S. Yan, and W. Liu, "An experimental research and analysis of the law of explosive stress wave propagation of cylindrical charge," *Applied Mechanics and Materials*, vol. 137, pp. 24–29, 2011.

[9] Y. H. Yoo, Y. Choi, J. Lee, and K. J. Yun, "Influence of the shape of explosive charge on the blast wave propagation," in *7th International Conference on Mechanical, Industrial, and Manufacturing Technologies*, Cape Town, South Africa, 2016.

[10] Z. D. Leng, W. B. Lu, M. Chen, P. Yan, and Y. G. Hu, "Improved the calculation model for the size of the crushed zone around the blasthole," *Explosion and Shock Waves*, 2015.

[11] H. Jang and E. Topal, "A review of soft computing technology applications in several mining problems," *Applied Soft Computing*, vol. 22, no. 6, pp. 38–51, 2014.

[12] D. E. Grady and M. E. Kipp, "Continuum modelling of explosive fracture in oil shale," *International Journal of Rock Mechanics and Mining Science and Geomechanics Abstracts*, vol. 17, no. 3, pp. 147–157, 1980.

[13] R. Yang, W. F. Bawden, and P. D. Katsabanis, "A new constitutive model for blast damage," *International Journal of Rock*

Mechanics and Mining ence & Geomechanics Abstracts, vol. 33, no. 3, pp. 245–254, 1996.

[14] G. W. Ma and X. M. An, "Numerical simulation of blasting-induced rock fractures," *International Journal of Rock Mechanics and Mining Sciences*, vol. 45, no. 6, pp. 966–975, 2008.

[15] A. Js, A. Tw, and B. Bl, "Practical assessment of rock damage due to blasting," *Science Direct International Journal of Mining Science and Technology*, vol. 29, no. 3, pp. 379–385, 2019.

[16] R. Holmberg and P. A. Persson, "The Swedish approach to contour blasting," *Proceedings of Conference on explosives and blasting technique*, Society of Explosives Engineers, New Orleans, 1978.

[17] W. Hustrulid and W. B. Lu, *Some General Concepts Regarding the Control of Blast-Induced Damage during Rock Slope Excavation*, 7th International symposium, rock fragmentation by blasting, Beijing: China, 2008.

[18] A. M. Starfield and J. M. Pugliese, "Compression waves generated in rock by cylindrical explosive charges: a comparison between a computer model and field measurements," *International Journal of Rock Mechanics and Mining Science and Geomechanics Abstracts*, vol. 5, no. 1, pp. 65–77, 1968.

[19] H. Li, X. Li, J. Li, X. Xia, and X. Wang, "Application of coupled analysis methods for prediction of blast-induced dominant vibration frequency," *Earthquake Engineering and Engineering Vibration*, vol. 15, no. 1, pp. 153–162, 2016.

[20] W. B. Lu, J. R. Zhou, M. Chen, P. Yan, and G. H. Wang, *Study on the Attenuation Formula of Dominant Frequency of Blasting Vibration*, Engineering Blasting, 2015.

[21] W. B. Lu, J. H. Yang, M. Chen, and C. Zhou, "An equivalent method for blasting vibration simulation," *Simulation Modelling Practice and Theory*, vol. 19, no. 9, pp. 2050–2062, 2011.

[22] Y. Hu, W. Lu, M. Chen, P. Yan, and J. Yang, "Comparison of blast-induced damage between presplit and smooth blasting of high rock slope," *Rock Mechanics and Rock Engineering*, vol. 47, no. 4, pp. 1307–1320, 2014.

[23] B. Xue, X. Du, J. Wang, and X. Yu, "A scaled boundary finite-element method with B-differentiable equations for 3D frictional contact problems," *Fractal and Fractional*, vol. 6, no. 3, p. 133, 2022.

[24] D. Liu, W. Lu, Y. Liu, M. Chen, P. Yan, and P. Sun, "Analysis of the main factors influencing the dominant frequency of blast vibration," *Shock and Vibration*, vol. 2019, 17 pages, 2019.

[25] Y. X. Peng, L. Wu, Y. Su, and C. H. Chen, "Study on the effect of elevation on the prediction of underwater drill and blasting vibration frequency," *Geosystem Engineering*, vol. 19, no. 4, pp. 170–176, 2016.

[26] A. H. Xayyraed, *Physical Process of Rock Blasting in Mining*, Mineral Press, Leningrad, 1974.